

Exploring water-level fluctuation amplitude in an approach channel under the regulation of a dual cascade hydro-plant in the dry season

Zhiyong Wan^{a,b}, Yun Li^{a,b,*}, Jianfeng An^b, Xiaogang Wang^b, Long Cheng^c and Yipeng Liao^{b,d}

^a School of Water Resources and Hydropower Engineering, Wuhan University, Wuhan 430072, China

^b State Key Laboratory of Hydrology-Water Resources and Hydraulic Engineering, Nanjing Hydraulic Research Institute, Nanjing 210029, China

^c Lower Changjiang River Bureau of Hydrology and Water Resources Survey, Changjiang Water Resources Commission, Nanjing 210011, China

^d College of Water Conservancy and Hydropower Engineering, Hohai University, Nanjing 210098, China

*Corresponding author. E-mail: yli@nhri.cn

ABSTRACT

Water-level fluctuation is a crucially important hydraulic factor to meet the safety of ship navigation. Due to the uncertainty and evolution of the maximum amplitude of water-level variation in the approach channel, the river reach between two dams located along the Yangtze River in China is selected as a study area and the impact of various operating conditions of the cascade hydro-plant on the maximum amplitude of water-level variation at typical sites is revealed combining the orthogonal test method and a hydrodynamic model. In addition, the critical threshold for the water-level variation at the lower lock head of the ship lift is explored using maximum entropy method. Results demonstrate that flow variation and regulation time are the most prominent factors affecting water-level fluctuation at the lower lock head of the ship lift, and the existing standard (0.5 m within 1 h and 0.3 m within 30 min) for controlling the maximum variation in water level at the lower lock head of the ship lift is reasonable and more safety oriented. This study provides a novel perspective to understand the response of water-level fluctuation to the stochasticity of operating conditions for the cascade hydropower stations.

Key words: approach channel, hydropower station, maximum entropy method, orthogonal experiment method, ship lift, water-level fluctuation

HIGHLIGHTS

- A one-dimensional hydrodynamic model was developed for validating the water-level fluctuation in the approach channel based on a physics model test.
- Using orthogonal array design method to address the intricate scenarios from the dual cascade hydropower stations.
- Using maximum entropy method (MEM) to examine the maximum water-level variation under the operation of large-scale cascade hydropower stations.

1. INTRODUCTION

Hydropower is the most vital source of renewable energy throughout the world and accounts for 19% of the planet's energy demand (Sharma & Singh 2013; Singh & Singal 2017). With an increase in demand for hydropower energy, hydropower stations have become increasingly ubiquitous on large rivers which have been channelized to allow for navigable flow conditions to a certain extent. Unsteady flow is a ubiquitous hydrodynamic phenomenon in the shallow shipping waterway and can yield a significant impact on downstream navigation, water supply and sediment transport (PIANC 1995; Ji *et al.* 2016; Zhang *et al.* 2018). Nevertheless, the flow pattern generated by the peaking-shaving operation of the hydropower stations (Xie *et al.* 2016), following the establishment of a hydro-plant has dramatically altered the hydraulic elements in the downstream river channel. Notably, water-level fluctuations have been recognized as a highly relevant indicator for shipping safety in the inland waterway navigation domain.

Water-level fluctuation generated during hydropower unit start-ups and shutdowns, with rapidly rising and falling of water level and the increment of the water surface gradient, can induce adverse navigation conditions in the waterway. Several relevant studies have been carried out to address this issue which focuses on the amplitude of water-level variations induced by the discharge regulation of hydropower plants, and therefore provide scientific and technological support for improving

This is an Open Access article distributed under the terms of the Creative Commons Attribution Licence (CC BY-NC-ND 4.0), which permits copying and redistribution for non-commercial purposes with no derivatives, provided the original work is properly cited (<http://creativecommons.org/licenses/by-nc-nd/4.0/>).

navigational conditions. In a previous study, [Zheng et al. \(2002\)](#) elucidated the effect of unsteady flow generated by the peaking of the hydropower station on the navigation conditions in the waterway between the Three Gorges Dam (TGD) and the Gezhouba Dam (GZD) located along the Yangtze River in China, and concluded that a counter-regulation mode of the GZD could control the navigation conditions in the relevant river sections within the limits allowed for shipping. Henceforth, numerous publications have reported the effect of unsteady flow generated by hydropower stations on navigational safety based on hydrological observations, numerical techniques, and physics model tests ([Li et al. 2006](#); [Liu et al. 2012](#); [Zhao et al. 2012](#); [Shang et al. 2017](#); [Jia et al. 2019](#)). These studies focused on the analysis of hydraulic elements in the waterway such as velocity, flow regime, water level and hydraulic gradient. However, the operation of the hydropower station involves the opening and closing of gates ([Tan et al. 2008](#)). On the one hand, the effects of transient processes of flow regulation on navigation have not been further considered; on the other hand, the stochastic combinations of various conditions during the joint operation of cascade hydropower stations have not been further reported in the literature.

In recent years, large-scale hydropower stations on the Yangtze River basin have been instrumental in enhancing the efficiency of China's hydropower energy, such as Wudongde, Baihetan, Xiluodu, Xiangjiaba, Three Gorges, and Gezhouba Hydropower Stations. Water-level fluctuations in the riverway during the dry season are mainly the result of various scheduling modes of hydropower stations. In the navigation domain, in addition to the navigation conditions in the waterway, the navigation conditions in an approach channel are increasingly highlighted ([Stockstill et al. 2004](#); [Maeck & Lorke 2014](#)). In particular, the safety of vessels in the approach channel is closely associated with water-level fluctuations. In general, surges induced by the regulation of hydropower stations during start-ups and shutdowns are the utmost crucial hydraulic parameters for assessing the navigation safety ([Bravo & Jain 1991](#)). In terms of the previous study on the Three Gorges approach channel, [Zhou et al. \(2005\)](#) revealed the influence of daily regulation of the Three Gorges Hydropower Station (TGHS) on water-level fluctuation in the upstream approach channel, such as load increment, load reduction, load rejection, and duration of units start-up as well as shutdown. Despite the current hydrographic and topographic data having altered over a long period, water-level fluctuation in the approach channel continues to be an important hot topic, especially at the lower lock head of the ship lift.

As an example of the daily operation of a system of cascade reservoirs, in this study, the river reach between the TGD and the GZD is selected and an attempt is made to investigate the probability density distribution based on the sample of maximum amplitude of water-level variation in the approach channel under the joint operation of the cascade hydropower stations. The main objective of this study is to gain a more in-depth understanding of the maximum water-level variation at the lower lock head of the ship lift during the dry period.

The remainder of this paper is organized as follows. Section 2 presents the description of the case studies, details of the numerical technique and model performance. Section 3 presents the results of the numerical validation, in terms of sample data of maximum amplitude of water-level variation obtained via one-dimensional hydrodynamic model and orthogonal array design method, and the threshold investigation of the maximum amplitude of water-level fluctuation at the lower lock head of the ship lift. Finally, the main conclusions drawn from this study are presented in Section 4.

2. MATERIALS AND METHODS

2.1. Description of the site

The Three Gorges Project (TGP) is located in the middle reaches of the Yangtze River, which is composed of a main dam, hydropower stations, and navigation structures with integrated functions of flood control, power generation, and navigation ([Zheng et al. 2018](#)). Notably, the TGHS and the Gezhouba Hydropower Station (GHS) constitute a typical cascade hydropower stations group. The TGHS has a rated output of 7,00,000 KW, with 32 units installed on the backside of the dam including 14 units on the left bank, 12 units on the right bank, and 6 units underground. In addition, there are another two 50,000 KW hydropower units, with a total installed capacity of 22.5 million KW. For the GHS, it has 2 units with a single capacity of 1,70,000 KW, and 19 units with a single capacity of 1,25,000 KW.

The main navigation structures of the TGP consist of a vertical ship lift and a dual-lane continuous five-step ship lock. For the approach channel of the ship lift, the riverbed width is around 80–90 m and the length of the channel is approximately 2,700 m. In particular, the approach channel of the ship lift merges with the approach channel approximately 1,100 m downstream of the ship lock, and then enters the main waterway of the Yangtze River. Following the confluence of the dual

approach channels (i.e., ship lift approach and ship lock approach), the entrance width is around 200 m, and the elevation of the riverbed is around 56.5 m. The arrangement of the entire approach channel is shown in Figure 1.

The river reach between the TGD and GZD starts from Yingzizui and ends at Wangjiagou the upstream of the GZD, which is about 38 km. The river section is mostly presented as U- or V-shaped in cross-section, with low velocity, excellent navigability, and minimum maintenance depth of 4.5 m during the dry season. The layout of the waterway between the TGD and the GZD is depicted in Figure 1.

2.2. One-dimensional hydrodynamic model

In the context of the long-distance river reach (around 38.0 km) between the TGD and the GZD, in this study, a one-dimensional hydrodynamic model in open channel flow between the TGD and the GZD was established using the Saint-Venant partial differential equations, that is, the continuity and momentum equations are herein as follows:

$$\text{Continuity equation: } B \frac{\partial Z}{\partial t} + \frac{\partial Q}{\partial x} = q \quad (1)$$

$$\text{Momentum equation: } \frac{\partial Q}{\partial t} + \frac{\partial (Q^2/A)}{\partial x} + gA \left(\frac{\partial Z}{\partial x} + \frac{Q|Q|}{K^2} \right) = 0 \quad (2)$$

where x is the coordinate along river length, m; t is the time, s; Q is the discharge, m^3/s ; B is the river width, m; Z is the water level, m; A is the flow area, m^2 ; q represents the source or sink, m^3/s ; g represents gravity acceleration, m/s^2 ; K represents the modulus of discharge.

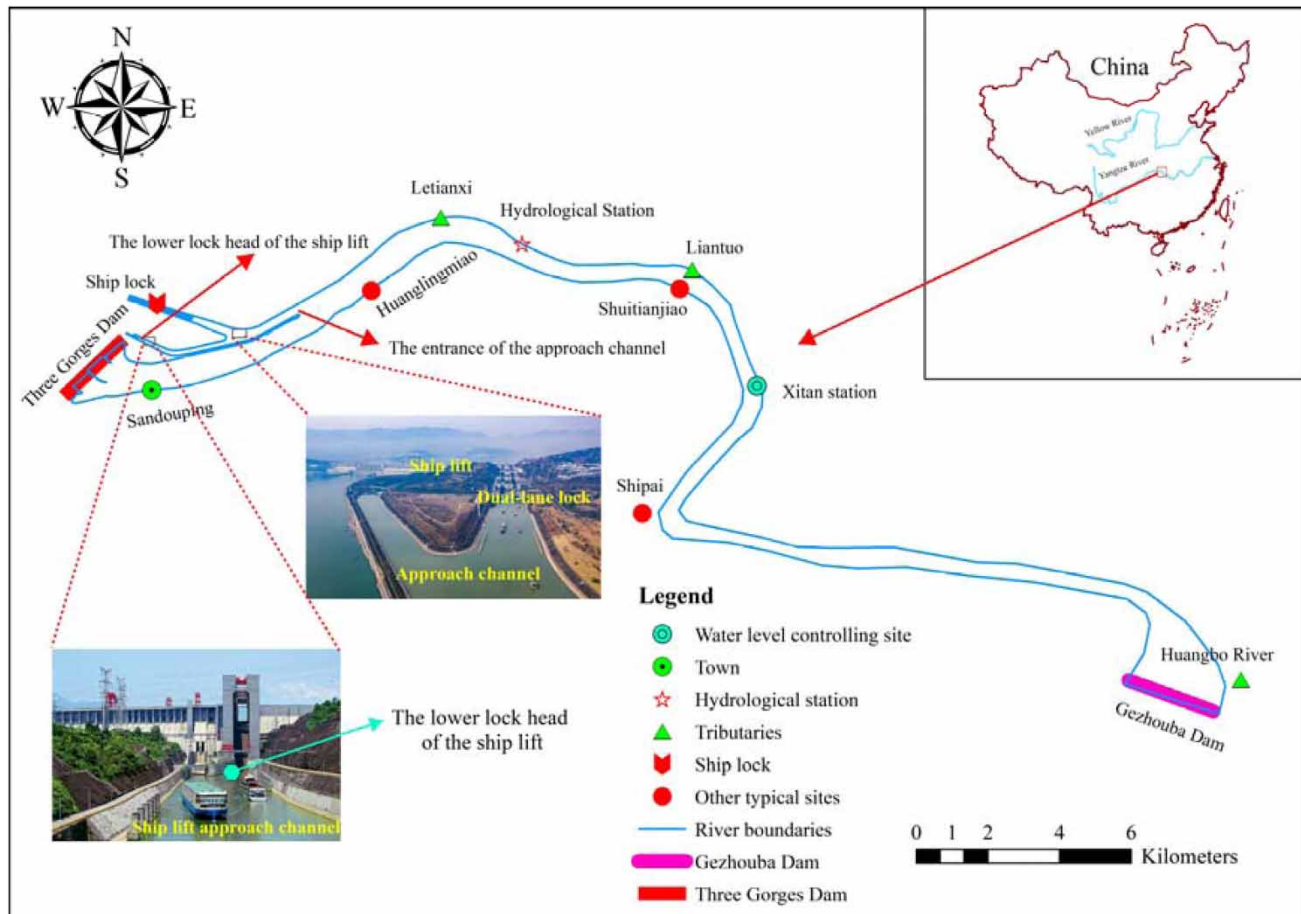


Figure 1 | Schematic views of the approach channel.

The aforementioned Saint-Venant equations are discretized using a Preissmann four-point implicit differentiation scheme and the difference form of the equations is written as (Cunge *et al.* 1980):

$$f(x, t) = \frac{\eta}{2}(f_{j+1}^{n+1} + f_j^{n+1}) + \frac{1-\eta}{2}(f_{j+1}^n + f_j^n) \quad (3)$$

$$\frac{\partial f}{\partial x} \approx \eta \frac{f_{j+1}^{n+1} - f_j^{n+1}}{\Delta x} + (1-\eta) \frac{f_{j+1}^n - f_j^n}{\Delta x} \quad (4)$$

$$\frac{\partial f}{\partial t} \approx \frac{f_{j+1}^{n+1} - f_{j+1}^n + f_j^{n+1} - f_j^n}{2\Delta t} \quad (5)$$

where η is the time-weighted coefficient, j and n represent the distance and number of time steps. In this study, η is set to 0.5, Δt is the time step set to 5 s, and the total simulation time is around 3 h. The cross-section of the study area is set every 5 m along the 38-km waterway for 7700 cross-sections in total from the TGD to the GZD.

2.3. Orthogonal experiment method

The issues of engineering practice are commonly influenced by multiple complex external and internal factors. In the actual engineering applications where numerous factors vary in a rather wide range, the conventional single factor method is considered to be time-consuming and cost demanding. However, orthogonal experiment method, as a statistical experimental design, is implemented to provide reliable and representative sample points from a comprehensive experiment based on orthogonality. In order to be capable of managing multi-factor trials in an efficient, quick and cost-effective manner, multiple factors and levels are first selected on the basis of the experience, then an orthogonal array with various numbers of factors and levels is obtained based on the work of Taguchi (Roy 2001); thereafter, the experiments can be conducted. Currently, this method is commonly utilized to analyze data sets based on the arrangement of levels and factors (Feng *et al.* 2017).

In this study, the maximum amplitude of water-level fluctuation is related to the operation mode of the dual hydropower units. Water-level fluctuations in the approach channel are influenced by multiple factors (e.g., the outflow boundary of the hydropower units varies from time to time), considering the advantages of the orthogonal experiment method, it is essential to identify the major factors using merely a fraction of possible operation scenarios of the dual hydropower units.

2.4. Maximum entropy fitting method (MEM)

The MEM is intended to be applied previously in engineering domains, and it specifies the most unbiased estimate of a probability distribution that maximizes the Shannon's entropy subject to the constraint information (Shannon 1948). In light of this, considering the relation between water-level fluctuations and the operating information of the hydropower units, a continuous random event upon the maximum amplitude of water-level fluctuation exhibited in the approach channel is expressed as:

$$H(p) = - \sum_{k=1}^n p_k \log p_k \quad (6)$$

where p_k denotes the probability of occurrence of a random event, $p_k > 0$ and $\sum p_k = 1$.

According to the maximum entropy principle (Abramov 2007; Chen *et al.* 2021), given the statistical moments of a sample as constraints, a constrained nonlinear optimization problem regarding the probability distribution of a random variable (y) is constructed as:

$$\begin{cases} \text{Find: } p(y) \\ \text{Maximize: } S(y) = - \int p(y) \ln(p(y)) dy \\ \text{Subject to } \begin{cases} \int p(y) dy = 1 \\ \int y^{\delta_i} p(y) dy = m_i^{\delta_i} \text{ for } i = 1, 2, \dots, N \end{cases} \end{cases} \quad (7)$$

where m_i is the δ_i -th moment of the random variable Z ; N is the number of moment constraints; $S(y)$ is the entropy defined in Equation (7).

The optimization problem in Equation (7) can be solved using the Lagrange multiplier method, and the general closed expression form of $p(y)$ such that:

$$p(y) = \exp\left(-\sum_{i=0}^N \lambda_i y^{\delta_i}\right) \quad (8)$$

where λ_i ($i = 0, 1, \dots, N$) represent the associated $M + 1$ Lagrange multipliers. The Equation (8) is substituted into the constraint condition in Equation (7), the initial values are written as:

$$\lambda_0 = \ln\left[\int \exp\left(-\sum_{i=1}^N \lambda_i y^{\delta_i}\right) dy\right] \quad (9)$$

For the given constraints, the constrained nonlinear optimization problem in Equation (7) could be transformed to the following set of unconstrained nonlinear optimization, that is,

$$\begin{cases} \text{Find: } \delta_i \& \lambda_i \ (i = 1, 2, \dots, N) \\ \text{Minimize: } \ell(\delta, \lambda) = \ln\left[\int \exp\left(-\sum_{i=1}^N \lambda_i y^{\delta_i}\right) dy\right] + \sum_{i=1}^N \lambda_i m^{\delta_i} \end{cases} \quad (10)$$

The exponential vector δ and Lagrange multipliers vector λ are solved via an efficient iterative method proposed by Gotovac and Gotovac (Volpe & Baganoff 2003), then the results are taken into Equation (9), and the coefficients of the probability density distribution are obtained.

2.5. Evaluation of model performance

To evaluate the accuracy of a one-dimensional hydrodynamic model in this study, four metrics are herein applied to identify the deviation between the measured data and the simulated one. Namely, Pearson Correlation Coefficient (R), Root Mean Square Error (RMSE), Mean Absolute Percentage Error (MAPE), and Nash-Sutcliffe Efficiency (NSE) are written as, respectively:

$$R = \frac{\sum_{i=1}^N (D_{mi} - \overline{D_m})(D_{si} - \overline{D_s})}{\sqrt{\sum_{i=1}^N (D_{mi} - \overline{D_m})^2 \sum_{i=1}^N (D_{si} - \overline{D_s})^2}} \quad (11)$$

$$RMSE = \sqrt{\frac{1}{N} \sum_{i=1}^N (D_{mi} - D_{si})^2} \quad (12)$$

$$MAPE = \frac{1}{N} \sum_{i=1}^N \frac{|D_{mi} - D_{si}|}{D_{mi}} \times 100\% \quad (13)$$

$$NSE = 1 - \frac{\sum_{i=1}^N (D_{si} - D_{mi})^2}{\sum_{i=1}^N (D_{mi} - \overline{D_m})^2} \quad (14)$$

where D_{mi} and D_{si} are the observed and simulated values for i th time step; N is the total number of samples; $\overline{D_m}$ and $\overline{D_s}$ are the mean of the observed and estimated values.

3. RESULTS AND DISCUSSION

3.1. Numerical validation of a one-dimensional hydrodynamic model

The navigable flow conditions in the approach channel under the combined operating conditions of the hydropower stations are relatively intricate, as a result of the water level in the approach channel oscillating back and forth in the form of a non-constant flow pattern. For simplicity, the main focus of this study is on water-level fluctuations at the entrance of the approach channel and the lower lock head of the ship lift. Assuming that the discharge outlets from both the TGHS and the GHS are set as flow boundaries, an overview of the typical load regulation mode for the cascade hydropower station is outlined as follows.

The discharge flow of $10,000 \text{ m}^3/\text{s}$ for the TGHS, the unit of the GHS increases by $3,000 \text{ m}^3/\text{s}$ for 5 min, and the discharge flow of the TGHS remains constant in a one-dimensional model and a physical model test at a 1:80 scale. The physical model is mainly composed of the hydropower stations, dam, ship lift approach channel, dual-lane ship lock approach channel, and the main channel (Figure 2). To investigate the water-level fluctuations in the approach channel, we conduct an experiment on the regulation of hydropower stations under the abovementioned condition. The typical locations of the lower lock head of the ship lift and the entrance of the approach channel are shown in Figure 2. The ratio of the water depth at k -th moment to the initial water depth (H_k/H_0) in the approach channel is selected as the dimensionless parameter for model validation. The comparison results of the physical model test and the numerical model in the approach channel are shown in Figure 3.

As shown in Figure 3, the established model is validated by comparing the simulated water depth with the measured one from a physics model test at a 1:80 scale. The error analysis results are shown in Table 1. MAPE varies from 0.664% to 1.539%, RMSE ranges from 0.050 to 0.091, and R as well as NSE vary from 0.958 to 0.996. Consequently, the good agreement between the model calculations and the measured data indicates that the established hydrodynamic model can accurately describe the water-level fluctuation in the approach channel, and it can be used for subsequent research.

3.2. Data-driven stochastic analysis of the influencing factors

Shallow water is characterized by significant hydrological fluctuation, particularly during the dry season, affecting the ship's navigation safety. Water-level fluctuation in the approach channel is related to the joint operation mode of the cascade

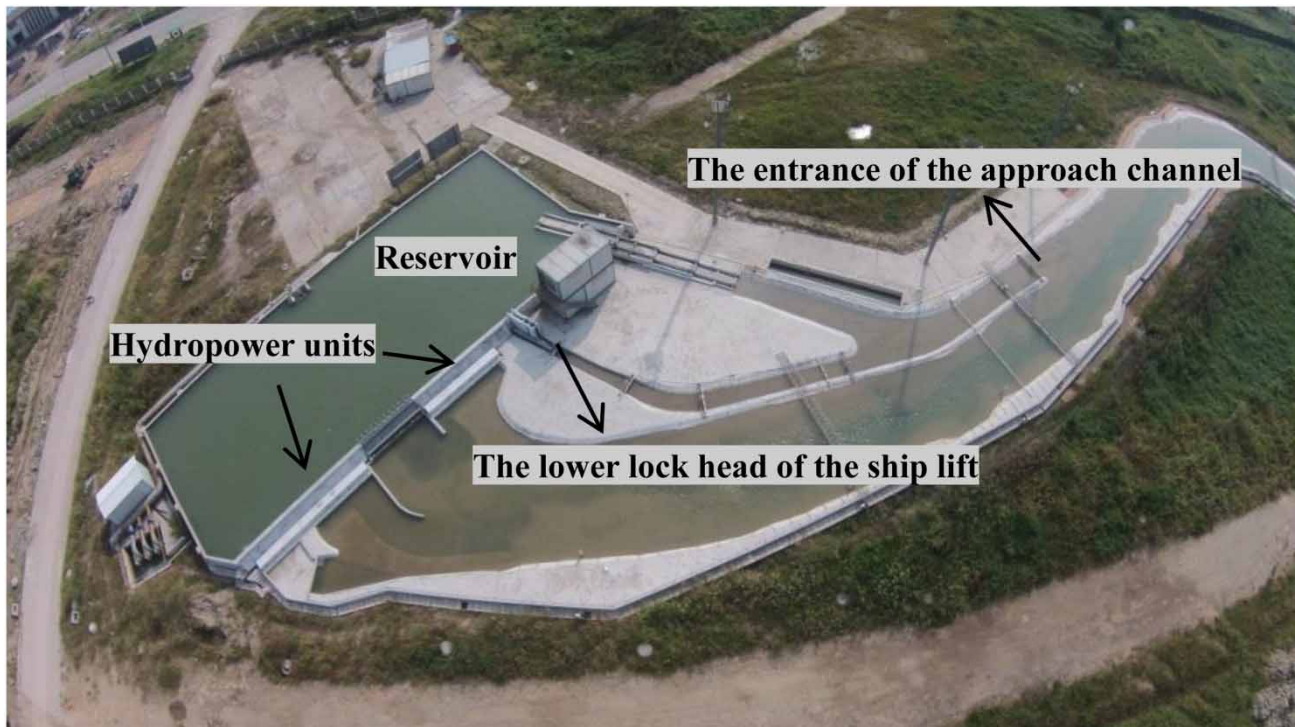


Figure 2 | A physical model layout of the approach channel.

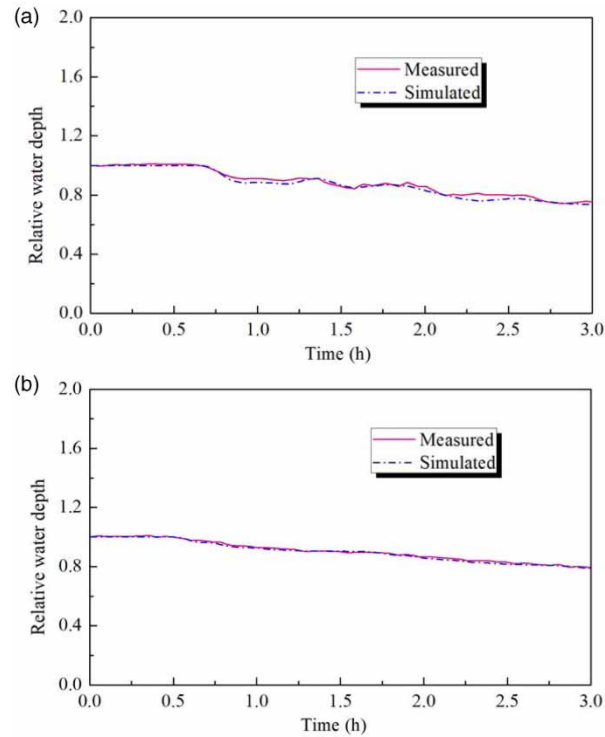


Figure 3 | Relative water depth (H_k/H_0) at typical sites in the approach channel. (a) Lower lock head of the ship lift. (b) The entrance of the approach channel.

Table 1 | Error analysis of model validation

Typical sampling sites	Validation			
	R	MAPE/%	RMSE/m	NSE
Lower lock head of the ship lift	0.987	1.539	0.091	0.958
The entrance of approach channel	0.996	0.664	0.050	0.988

hydropower stations. The maximum amplitude of water-level fluctuation in the waterway varies depending on operating conditions, and the unpredictability and ambiguity of water-level fluctuation directly threaten the navigational safety of vessels in the channel. For this reason, considering the boundary conditions of hydropower station operation during the dry season, initial water surface elevation, base flow, flow amplitude, and regulation time of hydropower stations are selected to conduct sensitivity analysis of the maximum water-level variation in the approach channel.

Due to the randomness of the operating scenarios of the hydropower units, it is extremely challenging to enumerate all the parameters with numerous samples. A multi-factor experiment design method, based on an orthogonal array $L_{27} (3^{13})$ designed with seven factors and three levels, is employed to generate effective samples of the boundary conditions upon the operation mode of the dual cascade hydropower stations, as presented in Tables 2 and 3. For simplicity, the range of parameters should be set to reflect the most unfavourable conditions during the dry season as far as possible: the range of the initial water surface elevation at the waterway between the TGD and the GZD is set to 64.0–65.0 m; the range of base flow is set to 5,000–6,000 m^3/s , the range of flow amplitude is set to 1,000–2,000 m^3/s , and the range of the regulation time of hydropower unit is set to 5–25 min. Factors and levels using orthogonal design of experiments are shown in Table 2.

Currently, in the engineering applications domain, the commonly available hydraulic indicators used to measure the magnitude of water-level fluctuations include maximum hourly variation and maximum daily variation. As the hourly variation indicator exhibits a tighter control on shipping safety, in light of this, the maximum amplitude of water-level fluctuation within 1 h is herein adopted.

Table 2 | Factors and levels of the orthogonal experiment

Factors	Level 1	Level 2	Level 3
Initial water surface elevation (m)	64.0	64.5	65.0
Base flow of the TGHS (m^3/s)	5,000	5,500	6,000
Flow amplitude of the TGHS (m^3/s)	1,000	1,500	2,000
Control time of the TGHS (min)	5	15	25
Base flow of the GHS (m^3/s)	5,000	5,500	6,000
Flow amplitude of the GHS (m^3/s)	1,000	1,500	2,000
Control time of the GHS (min)	5	15	25

Table 3 | Summary of the $L_{27} (3^{13})$ orthogonal array

Trials	W (m)	B1 (m^3/s)	A1 (m^3/s)	T1 (min)	B2 (m^3/s)	A2 (m^3/s)	T2 (min)	E (m)	F (m)
1	64.0	5,000	1,000	5	5,000	1,000	5	0.16	0.37
2	64.0	5,000	1,000	5	5,500	1,500	15	0.34	0.49
3	64.0	5,000	1,000	5	6,000	2,000	25	0.51	0.71
4	64.0	5,500	1,500	15	5,000	1,000	5	0.26	0.40
5	64.0	5,500	1,500	15	5,500	1,500	15	0.21	0.38
6	64.0	5,500	1,500	15	6,000	2,000	25	0.37	0.53
7	64.0	6,000	2,000	25	5,000	1,000	5	0.43	0.55
8	64.0	6,000	2,000	25	5,500	1,500	15	0.29	0.49
9	64.0	6,000	2,000	25	6,000	2,000	25	0.24	0.38
10	64.5	5,000	1,500	25	5,000	1,500	25	0.19	0.28
11	64.5	5,000	1,500	25	5,500	2,000	5	0.43	0.62
12	64.5	5,000	1,500	25	6,000	1,000	15	0.32	0.43
13	64.5	5,500	2,000	5	5,000	1,500	25	0.32	0.58
14	64.5	5,500	2,000	5	5,500	2,000	5	0.31	0.71
15	64.5	5,500	2,000	5	6,000	1,000	15	0.30	0.50
16	64.5	6,000	1,000	15	5,000	1,500	25	0.19	0.38
17	64.5	6,000	1,000	15	5,500	2,000	5	0.25	0.41
18	64.5	6,000	1,000	15	6,000	1,000	15	0.13	0.22
19	65.0	5,000	2,000	15	5,000	2,000	15	0.28	0.46
20	65.0	5,000	2,000	15	5,500	1,000	25	0.26	0.36
21	65.0	5,000	2,000	15	6,000	1,500	5	0.41	0.73
22	65.0	5,500	1,000	25	5,000	2,000	15	0.24	0.33
23	65.0	5,500	1,000	25	5,500	1,000	25	0.11	0.18
24	65.0	5,500	1,000	25	6,000	1,500	5	0.35	0.48
25	65.0	6,000	1,500	5	5,000	2,000	15	0.25	0.55
26	65.0	6,000	1,500	5	5,500	1,000	25	0.26	0.48
27	65.0	6,000	1,500	5	6,000	1,500	5	0.22	0.52

Maximum amplitudes of water-level fluctuations at the entrance of the approach channel and the lower lock head of the ship lift, according to the design sample, are readily obtained using a one-dimensional hydrodynamic model. As shown in Table 3, W represents initial water surface elevation; B1, A1, and T1 represent base flow, flow amplitude, and regulation

time of the TGHS, respectively; B2, A2, and T2 represent base flow, flow amplitude, and regulation time of the GHS, respectively. E and F denote the maximum hourly amplitude of water level at the entrance of the approach channel and the lower lock head of the ship lift, respectively. In combination with running conditions for the hydropower units, the maximum amplitudes of water-level fluctuations within 1 h at the entrance of the approach channel and the lower lock head of the ship lift under various scenarios are presented in Table 3. Specifically, the maximum amplitude of water-level fluctuation within 1 h at the lower lock head of the ship lift is recorded in the 21st experiment trials, such as 0.73 m, whereas the one at the entrance of the approach channel is recorded in the third experiment trials, such as 0.51 m.

As presented in Tables 3–5, the values of F and E are obtained by the hydrodynamic model based on the given boundary conditions. According to the principle of the orthogonal experimental design, F_i ($i = 1, 2, 3$) is defined as the average value of the evaluation index F for each factor at the same level; while E_i ($i = 1, 2, 3$) is defined as the average value of the evaluation index E for each factor at the same level. R_S is defined as the range between the maximum F value and the minimum F value in the corresponding factor; while R_E is defined as the range between the maximum E value and the minimum E value in the corresponding factor.

As presented in Table 4 and Figure 4, according to the analysis of variance results, the regulation time of the TGHS and the flow amplitude of the GHS are recognized to be the most effective factors playing a pivotal role in terms of the maximum hourly amplitude of water level at the lower lock head of the ship lift. Namely, the shorter the flow regulation time of the TGHS, the greater the water-level fluctuation will be at the lower lock head of the ship lift; the water-level fluctuation will be more significant with an increase in flow amplitude of the GHS. In addition, as the initial water surface elevation and base flow of the TGHS grows, the maximum water-level fluctuation amplitude at the lower lock head of the ship lift decrease gradually; with an increment of flow amplitude of the TGHS and the GHS, the maximum water-level fluctuation amplitude at the lower lock head of the ship lift is more significant; the flow regulation with shorter time of the GHS and the TGHS exerts a significant impact on the maximum water-level fluctuation. In particular, with an increment of base flow for the GHS, the maximum water-level fluctuation amplitude increases gradually. Overall, flow amplitude and regulation time are the most significant factors for the water-level fluctuation amplitude at the lower lock head of the ship lift.

Table 4 | Response table for means (maximum hourly amplitude of water level at the lower lock head of the ship lift, unit: m)

Factors	F1 (Level 1)	F2 (Level 2)	F3 (Level 3)	R_S
Initial water surface elevation (W)	0.48	0.46	0.46	0.02
Base flow of the TGHS (B1)	0.49	0.45	0.44	0.05
Flow amplitude of the TGHS (A1)	0.46	0.47	0.53	0.07
Regulation time of the TGHS (T1)	0.55	0.43	0.42	0.13
Base flow of the GHS (B2)	0.43	0.46	0.50	0.07
Flow amplitude of the GHS (A2)	0.39	0.48	0.52	0.13
Regulation time of the GHS (T2)	0.53	0.43	0.43	0.10

Table 5 | Response table for means (maximum hourly amplitude of water level at the entrance of approach channel, unit: m)

Factors	E1 (Level 1)	E2 (Level 2)	E3 (Level 3)	R_E
Initial water surface elevation (W)	0.31	0.27	0.26	0.05
Base flow of the TGHS (B1)	0.32	0.28	0.25	0.07
Flow amplitude of the TGHS (A1)	0.25	0.28	0.32	0.07
Regulation time of the TGHS (T1)	0.30	0.26	0.28	0.04
Base flow of the GHS (B2)	0.26	0.27	0.32	0.06
Flow amplitude of the GHS (A2)	0.25	0.28	0.32	0.07
Regulation time of the GHS (T2)	0.31	0.26	0.26	0.05

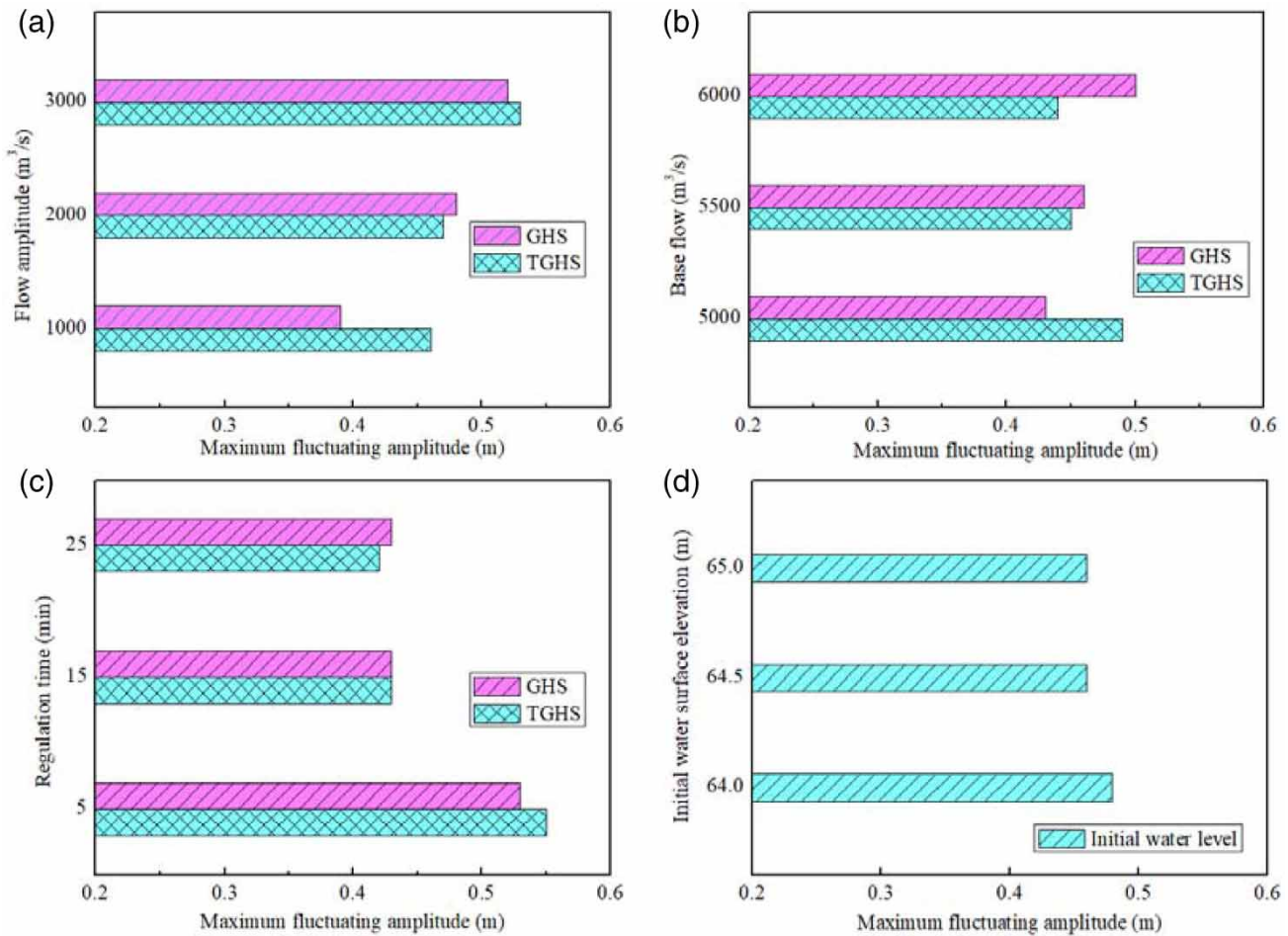


Figure 4 | Influence of various factors on the maximum water-level fluctuation amplitude at the lower lock head of the ship lift. (a) Flow amplitude; (b) base flow; (c) regulation time of the hydropower units; (d) initial water surface elevation.

Additionally, the maximum hourly amplitude of water level at the entrance of the approach channel is presented in Table 5. As the entrance is situated at the confluence of the approach channel and the main waterway, the water-level fluctuation in the main waterway is similar to that at the entrance of the approach channel. Results indicate that the flow amplitude of the TGHS and the GHS is the most significant influencing factor at the entrance of the approach channel. In addition, base flow is recognized as the secondary factor, and the regulation time of the hydropower unit is not significant. Compared with water-level fluctuation at the lower lock head of the ship lift, flow regulation time of the hydropower unit may induce insignificant water-level fluctuation in the wider reaches, whereas the amplitude of water-level variation at the narrower river sections exhibits a greater change.

The maximum amplitude of water-level variation may vary with downstream hydrographic data and the safe docking pattern of the ship lift chamber. Consequently, to illustrate fully the maximum water-level variation at the lower lock head of the ship lift, according to the potential operation scenarios of the cascade hydropower stations in Table 3, the maximum amplitudes of water-level variation within the periods of 5, 10, 15, 20, 30, and 60 min at the lower lock head of the ship lift and the entrance of the approach channel are shown in Figure 5.

As presented in Figure 5(a) and 5(b), most of the simulated values of the water-level variation at the lower lock head of the ship lift and the entrance of the approach channel are concentrated between the 25th and the 75th percentile of the corresponding distributions, and the medians are close to the means with an upward trend. Overall, the water level at the lower lock head of the ship lift fluctuates considerably due to the effect of the narrowing of the hydraulic section, and the average water-level variation within 1 h is slightly below the existing design threshold of 0.5 m based on the navigation standard (MOT 2018) of the two dams located along the Yangtze River in China. There is a potential risk for the operation

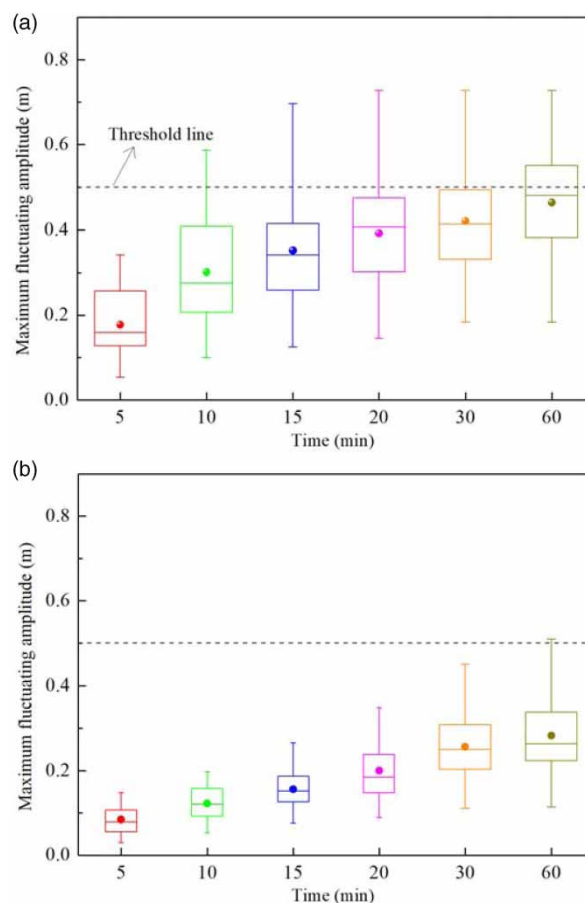


Figure 5 | Maximum water-level fluctuation amplitude within various periods. (a) The lower lock head of the ship lift; (b) The entrance of the approach channel.

of the ship lift, the maximum amplitude of water-level variation at the lower lock head of the ship lift will be therefore a major concern.

3.3. Threshold investigation of maximum water-level fluctuation amplitude

The safe docking of the ship chamber at the lower lock head of ship lift is closely associated with the water-level fluctuation (e.g., too low water level with a risk of the ship grounding, too high water level with overflowing from the ship chamber) in the approach channel, thus water-level fluctuations in the vicinity of the lower lock head of the ship lift should be a major concern.

To ensure navigation safety of ships, in consideration of the requirements for safe docking of the Three Gorges ship lift chamber, the existing critical threshold of the water-level fluctuation amplitude within 1 h at the lower lock head of the ship lift is set to 0.5 m (MOT 2018), which is utilized to monitor the water-level fluctuation in the approach channel. In this regard, it is pretty crucial for the safe docking of the ship chamber as the ship lift is under operation. However, the critical threshold is associated with the changes in hydrologic regimes induced by downstream junction scheduling. Maximum water-level fluctuation amplitude in the approach channel is primarily affected by base flow, flow amplitude, regulation time of hydropower units, and initial water surface elevation. Currently, the randomness of the outflow boundary of the hydropower units is tough to capture precisely, and the maximum water-level fluctuation amplitude in the approach channel induced by the operation of the hydropower units is not clearly understood by the shipping community. Accordingly, in this subsection, an attempt to adopt a novel perspective to identify the critical threshold of water-level fluctuation amplitude is herein proposed via probability density distribution among scenarios from the regulation modes of the TGHS and the GHS.

3.3.1. Synchronous and asynchronous peaking of cascade hydropower stations

To fully reflect the influence of the variation of the operating conditions of the cascade hydropower stations on the amplitude of the water-level variation at the lower lock head of the ship lift, all the potential regulation scenarios of the hydro-plant (Table 3) are considered in detail.

Taking the maximum water-level fluctuation amplitude within 1 h as a case, the maximum water-level fluctuation amplitude for each scenario in Table 3 is obtained using a hydrodynamic model, and the distribution of probability density function based on the sample data composed of maximum water-level fluctuation amplitude for all scenarios in Table 3 is computed by Equations (7)–(10). Simultaneously, a fully non-parametric test method, named the Kolmogorov–Smirnov (K-S) test method, is used to compare with that of the results from the maximum entropy method (MEM).

For the pattern of the probability density distribution, the conventional K-S test method is a versatile tool to examine the potential distribution pattern, whereas it is not essential to assume the distribution function type of samples before a test using the moment-constrained MEM. In terms of the moments, the probability density distributions with moment constraints of order up to 4, 5 and 6 are selected, respectively, and presented in Figure 6.

As shown in Figure 6, the probability density distribution of the maximum amplitude of water-level variation at the lower lock head of the ship lift agrees well with that of the conventional K-S method, especially the result of the 4th order moment is closer to the distribution pattern of K-S method ($R = 0.998$, $NSE = 0.997$, and $RMSE = 0.053$). Accordingly, on the basis of the validation result of the existing model, the probability distribution of the maximum amplitude of water-level variation

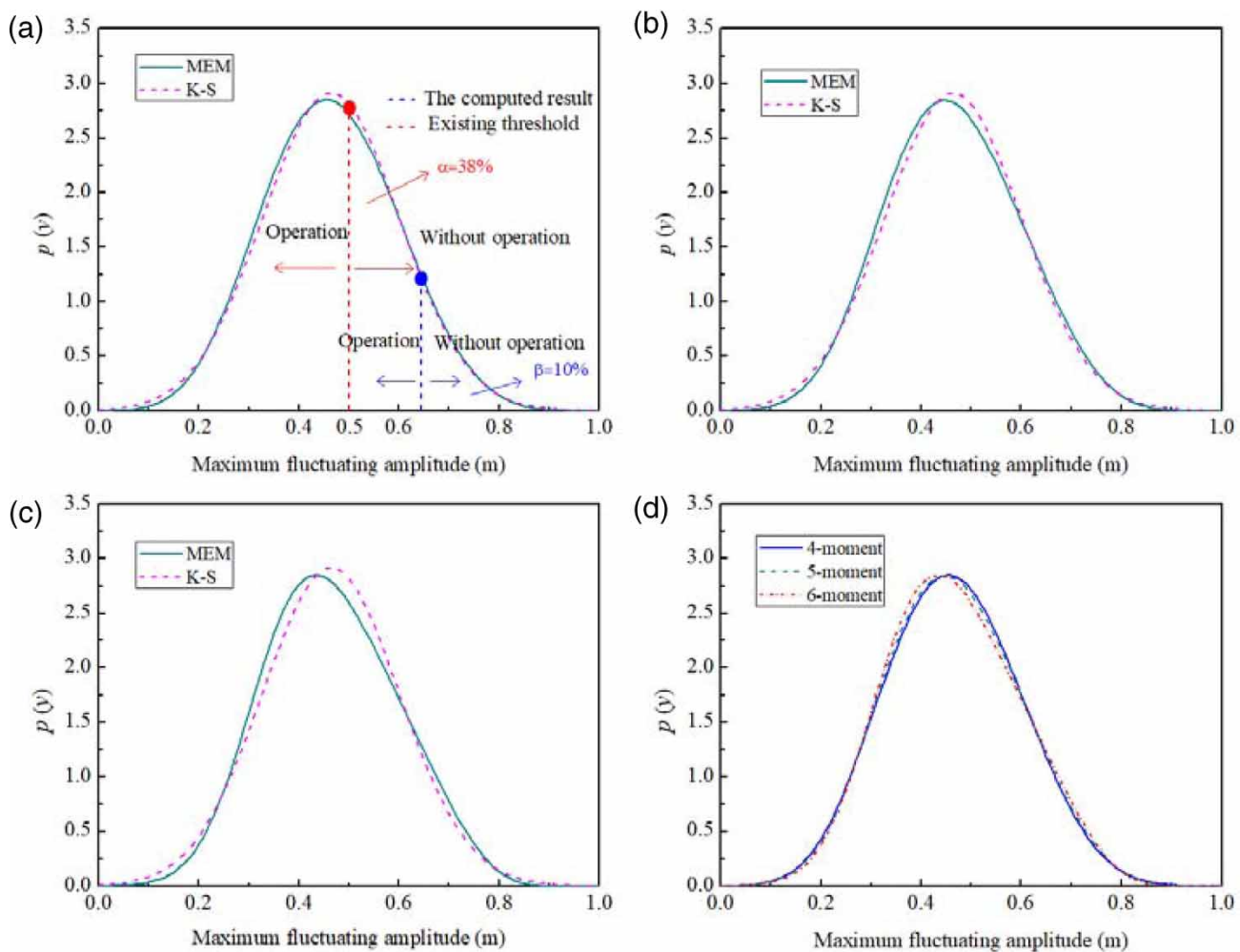


Figure 6 | Distributions of maximum water-level fluctuation amplitude. (a) 4-moment; (b) 5-moment; (c) 6-moment; (d) comparison of various moments.

at the lower lock head of the ship lift for each dispatching mode of the hydropower units can be described precisely using the moment constraints of order up to 4.

It is known that the normal operation of the Three Gorges ship lift is closely related to the variation of the water level at the lower lock head of the ship lift. To ensure the safe navigation of the ship lift, the maximum water-level variation within 1 h at the lower lock head of the ship lift is limited to 0.5 m. According to the probability density distribution of the maximum water-level fluctuation amplitude (Figure 6(a)), the probability that the water-level fluctuation at the lower lock of the ship lift fails to meet the safe navigation of ship is around 38% when the maximum amplitude of water-level variation reaches 0.5 m. Totally, the majority of operating conditions for the cascade hydropower stations meet the requirement for safe docking of the ship lift chamber.

Additionally, the sample aforementioned encompasses the calculated values for the least favourable conditions of the cascade hydropower stations during the dry season; on the contrary, provided that the entire scheduling modes of the cascade hydropower stations are in accordance with the normal operating conditions, the safe navigation guarantee rate of the ship lift during the dry period should be higher. For instance, according to the prototype observations in 2019, the probability of the maximum water-level variation at the lower lock head of the ship lift not being satisfied for each month is around 2–10%. It is apparent that the docking of the ship lift chamber is in a safe condition during most of the dry season, that is, the maximum variation of the water level at the lower lock head of the ship lift is within the safety threshold. In addition, assuming a 10% probability (stem from prototype observation data) of failing to satisfy the maximum amplitude of the water-level variation at the lower lock head of the ship lift, the critical threshold for the hourly variation of the water level is 0.64 m, whereas the existing maximum amplitude of the water-level variation at the lower lock head of the ship lift is determined to be 0.5 m within 1 h. Therefore, existing regulations have a stricter requirement for controlling the maximum hourly variation in water level at the lower head of the ship lift, and the existing standard is more safety-oriented.

3.3.2. Simultaneous peaking of cascade hydropower stations

In terms of the simultaneous peaking of cascade hydropower stations, the sample can be constructed using the trails series composed of the numbers 1, 5, 9, 10, 14, 18, 19, 23, and 27 in Table 3. These samples present the potential operating scenarios for simultaneous peaking of the cascade hydropower stations with the same initial water level, base flow, flow amplitude, and flow regulation time, as shown in Table 6.

The sample of maximum water-level fluctuation amplitude within 1 h at the lower lock head of the ship lift is listed in the last column of Table 6. Assuming the probability of 10% of unsafe navigation, the critical threshold of the maximum hourly water level amplitude at the lower lock head of the ship lift was determined to be 0.61 m based on the MEM, whereas the actual threshold (0.5 m, Figure 7) is less than the previous one. Hence, it indicates that the existing standard is more stringent for the safe docking of the ship chamber at the lower lock head of the ship lift and that the safe passage of the ship under the simultaneous regulation of the cascade hydropower stations is guaranteed at a high rate.

Table 6 | Potential scenarios for the simultaneous peaking of cascade power stations

ss	W (m)	B1 (m ³ /s)	A1 (m ³ /s)	T1 (min)	B2 (m ³ /s)	A2 (m ³ /s)	T2 (min)	F (m)	G (m)
1	64.0	5,000	1,000	5	5,000	1,000	5	0.37	0.36
5	64.0	5,500	1,500	15	5,500	1,500	15	0.38	0.38
9	64.0	6,000	2,000	25	6,000	2,000	25	0.38	0.38
10	64.5	5,000	1,500	25	5,000	1,500	25	0.28	0.28
14	64.5	5,500	2,000	5	5,500	2,000	5	0.71	0.71
18	64.5	6,000	1,000	15	6,000	1,000	15	0.22	0.22
19	65.0	5,000	2,000	15	5,000	2,000	15	0.46	0.46
23	65.0	5,500	1,000	25	5,500	1,000	25	0.18	0.18
27	65.0	6,000	1,500	5	6,000	1,500	5	0.52	0.51

Note: F denotes the maximum water-level variation within 60 min at the lower lock head of the ship lift, while G represents the maximum water-level variation within 30 min at the lower lock head of the ship lift; and the remaining symbols have the same meaning as previously mentioned.

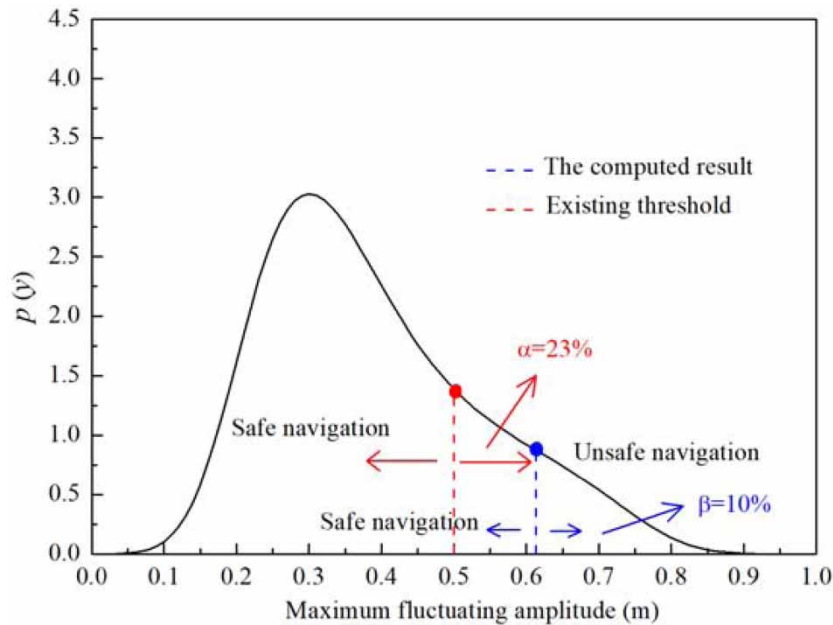


Figure 7 | Distribution of maximum amplitude of the water-level variation within 60 min at the lower lock head of the ship lift.

3.4. Discussions

The threshold of water-level variation at the lower lock head of the ship lift is related to the safe docking mode of the ship chamber, and the magnitude of the water-level variation is directly associated with the evolution of the river topography and the scheduling modes of the cascade hydropower stations. Nevertheless, the existing standard of water-level variation at the lower lock head of the ship lift is based on a relatively vague source, and the adoption of a more strict threshold of water-level variation considerably restricts the enhancement of the navigational security rate of the ship lift, resulting in the ship lift's navigational efficiency not being given full play; conversely, the threshold of water-level variation is taken too roughly in range, which will increase the possibility of navigational safety risks for ships. However, in terms of engineering applications, as long as the ships can be safely docked at the lower lock head of the ship lift, the current maximum amplitude of water-level fluctuation can be considered to be satisfied. Although prototype observation tests are the best means of reflecting water-level fluctuations at the lower lock head of the ship lift, there are risks associated with such means. In light of this, it is meaningful to investigate the threshold value of water-level fluctuation amplitude at the lower lock head of the ship lift.

3.4.1. Maximum water-level variation within 30 min

Currently, the threshold of the maximum amplitude of water-level fluctuation is determined to be 0.5 m within 1 h, is it feasible to adopt other standards for the safe docking of ships at the lower lock head of the ship lift? In light of this, assuming that the threshold value of water-level variation at the lower lock head of the ship lift should be 0.3 m within 30 min during the dry season, the sample information concerning the maximum water-level variation with 30 min could be obtained using 27 sets of scenarios available (Table 3). The probability distribution of the maximum amplitude of water-level variation at the lower lock head of the ship lift is shown in Figure 8.

As shown in Figure 8(a), assuming the probability of 50% of unsafe navigation, the critical threshold of the maximum hourly water level amplitude at the lower lock head of the ship lift is determined to be 0.40 m based on the MEM, which is greater than the actual threshold value (0.3 m within 30 min). However, the abnormal probability of safe navigation corresponding to the threshold standard is around 81%. Overall, the existing threshold of maximum water-level variation within 30 min is more safety oriented.

Likewise, assuming the unsafe probability of 50%, the critical threshold of the maximum amplitude of water-level fluctuation at the lower lock head of the ship lift is regarded as 0.36 m, which is greater than the actual threshold value (0.3 m, Figure 8(b)). Further, the probability of unsafe navigation corresponding to the existing standard is around 68%. In general,

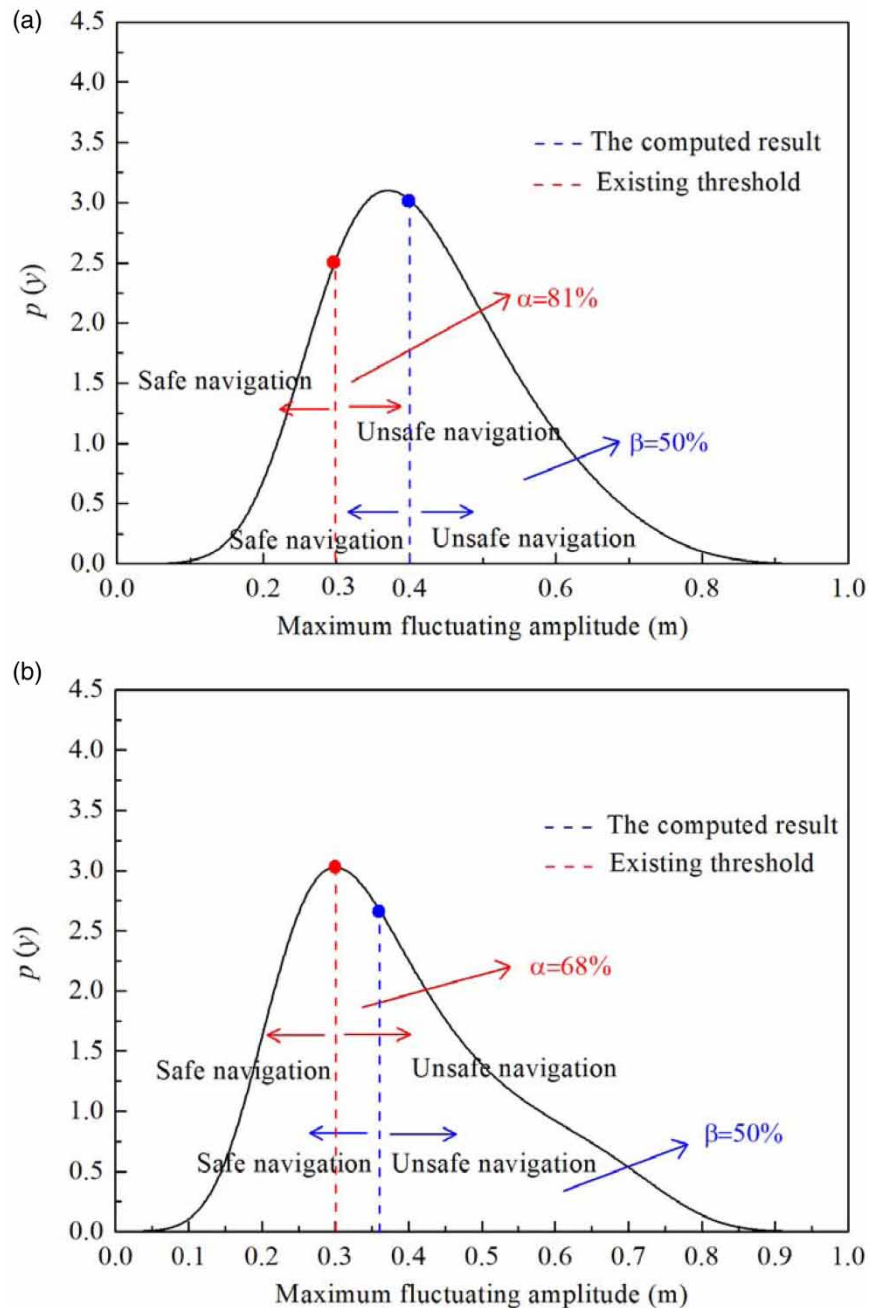


Figure 8 | Distribution of maximum amplitude of the water-level variation within 30 min at the lower lock head of the ship lift. (a) Synchronous and asynchronous peaking of the dual cascade hydropower stations. (b) Simultaneous peaking of the dual cascade hydropower stations.

when water-level fluctuation amplitude is computed based on a standard of 0.3 m within 30 min, the existing standard is more stringent for the safe docking of the ship chamber at the lower lock head of the ship lift.

3.4.2. Shortcomings and future work

The maximum water-level variation at the lower lock head of the ship lift is not only related to the safe docking of vessels but also to the changing hydrologic regimes between the TGD and the GZD during the scheduling of the dual cascade hydropower stations. This study examines the critical threshold of water-level variation amplitude in the approach channel

merely in terms of the hydrologic regimes between the TGD and the GZD under the cascade hydropower stations schedule. Nevertheless, several shortcomings in this study are as follows: (i) a small sample containing the least favourable combination of conditions is utilized to determine the distribution of probability density function; and (ii) water-level fluctuation at the lower lock head of the ship lift under the load-increasing operation of hydropower unit is merely taken into consideration, while the combination conditions of load-decreasing, load-increasing, and a constant load of the hydropower unit are not further discussed. Overall, the sample information in this study has a few limitations. In future work, prototype observation and experimental data upon water-level fluctuation at the lower lock head of the ship lift under various operating modes of the cascade hydropower stations will be further gathered and analyzed using the statistical method and machine learning algorithms.

4. CONCLUSION

Considering the uncertainty of the threshold of the maximum water-level variation at the lower lock head of the ship lift, in this study, a one-dimensional hydrodynamic model was numerically solved to obtain water-level fluctuation amplitude at typical cross-sections, then the orthogonal experiment method was adopted to reduce the number of factors influencing the involved processes to a limited number of combinations. In light of this, the MEM was employed to obtain the occurrence probability of the maximum amplitude of water-level fluctuation in consideration of the stochastic combination of operating operations of the dual cascade hydropower stations. The following conclusions can be drawn from this study: (i) The established one-dimensional hydrodynamic model is effective and reliable in water-level fluctuation simulating. (ii) Flow amplitude and regulation time of the unit are the most significant factors for the amplitude of water-level variation at the lower lock head of the ship lift, and flow amplitude is the most prominent factor affecting the amplitude of water-level variation at the entrance of approach channel. (iii) The probability density distribution of the maximum amplitude of water-level fluctuation at the lower lock head of the ship lift is capable of being obtained using the MEM, and it indicates that the existing standard (0.5 m within 1 h and 0.3 m within 30 min) for controlling the maximum hourly variation in water level at the lower lock head of the ship lift is reasonable and more safety oriented.

ACKNOWLEDGEMENTS

This research was jointly funded by the National Key Research and Development Program of China (2016YFC0401906) and the Three Gorges Follow-up Work Research Project (SXXTD-2018-8).

CONFLICTS OF INTEREST

The authors declare that they have no conflicts of interest.

DATA AVAILABILITY STATEMENT

All relevant data are included in the paper or its Supplementary Information.

REFERENCES

- Abramov, R. V. 2007 [An improved algorithm for the multidimensional moment-constrained maximum entropy problem](#). *Journal of Computational Physics* **226**, 621–644.
- Bravo, H. R. & Jain, S. C. 1991 [Flow fields in lower lock approaches induced by hydro-plant releases](#). *Journal of Waterway, Port, Coastal, and Ocean Engineering* **117**, 369–389.
- Chen, B.-Y., Kou, Y., Zhao, D., Wu, F., Wang, L.-P. & Liu, G.-L. 2021 [Maximum entropy distribution function and uncertainty evaluation criteria](#). *China Ocean Engineering* **35** (2), 238–249.
- Cunge, J. A., Holly, F. M. & Verwey, A. 1980 *Practical Aspects of Computational River Hydraulics*. Pitman Publishers, Ltd., London, England.
- Feng, Z.-K., Niu, W.-J., Cheng, C.-T. & Liao, S.-L. 2017 [Hydropower system operation optimization by discrete differential dynamic programming based on orthogonal experiment design](#). *Energy* **126**, 720–732.
- Ji, U., Jang, E.-K. & Kim, G. 2016 [Numerical modelling of sedimentation control scenarios in the approach channel of the Nakdong River Estuary Barrage, South Korea](#). *International Journal of Sediment Research* **31** (3), 257–263.
- Jia, T., Qin, H., Yan, D., Zhang, Z., Liu, B., Li, C., Wang, J. & Zhou, J. 2019 [Short-term multi-objective optimal operation of reservoirs to maximize the benefits of hydropower and navigation](#). *Water* **11** (6), 1272.
- Li, F., Yang, W. & Dai, H. 2006 Research on the influence of unsteady flow produced by the operation of TGP on navigation III: lower Yichang reach of Gezhouba project. *Journal of Hydroelectric Engineering* **25** (1), 56–60 (in Chinese).

- Liu, Z., Ma, A. & Cao, M. 2012 Shuifu-Yibin channel regulation affected by unsteady flow released from Xiangjiba Hydropower Station. *Procedia Engineering* **28**, 18–26.
- Maecck, A. & Lorke, A. 2014 Ship-lock-induced surges in an impounded river and their impact on subdaily flow velocity variation. *River Research and Applications* **30** (4), 494–507.
- MOT (Ministry of Transport). Changjiang River Administration of Navigational Affairs 2018 *Three Gorges-Gezhouba Water Conservancy Hub Navigation Scheduling Regulations*. Wuhan, China (in Chinese).
- PIANC (MarCom Working Group 30) 1995 *Joint PIANC-IAPH Report on Approach Channels–Preliminary Guidelines: Supplement to Bulletin no. 87*. PIANC General Secretariat, Brussels, Belgium.
- Roy, R. K. 2001 *Design of Experiments Using the Taguchi Approach: 16 Steps to Product and Process Improvement*. John Wiley & Sons, New York. pp. 98–102.
- Shang, Y., Li, X., Gao, X., Guo, Y., Ye, Y. & Shang, L. 2017 Influence of daily regulation of a reservoir on downstream navigation. *Journal of Hydrologic Engineering* **22** (8), 05017010.
- Shannon, C. E. 1948 *A mathematical theory of communication*. *The Bell System Technical Journal* **27** (3), 379–423.
- Sharma, H. & Singh, J. 2013 Run off river plant: status and prospects. *International Journal of Innovative Technology and Exploring Engineering* **3** (2), 210–213.
- Singh, V. K. & Singal, S. K. 2017 Operation of hydro power plants-a review. *Renewable and Sustainable Energy Reviews* **69**, 610–619.
- Stockstill, R. L., Park, H. E., Hite, J. E. & Shelton, T. W. 2004 *Design Considerations for Upper Approaches to Navigation Locks*. U.S. Army Engineer Research and Development Center, Vicksburg, MS.
- Tan, G.-M., Ding, Z.-L., Wang, C.-D. & Yao, X. 2008 Gate regulation speed and transition process of unsteady flow in channel. *Journal of Hydrodynamics* **20** (2), 231–238.
- Volpe, E. V. & Baganoff, D. 2003 Maximum entropy pdfs and the moment problem under near-Gaussian conditions. *Probabilistic Engineering Mechanics* **18**, 17–29.
- Xie, M., Zhou, J., Li, C. & Lu, P. 2016 Daily generation scheduling of cascade hydro plants considering peak shaving constraints. *Journal of Water Resources Planning and Management* **142** (4), 04015072.
- Zhang, Z., Qin, T., Wang, H., Lei, X.-H., Tian, Y. & Lu, L.-B. 2018 Numerical analysis of the hydraulic transient process of the water delivery system of cascade pump stations. *Water Supply* **18** (5), 1635–1649.
- Zhao, J., Zhao, S. & Cheng, X. 2012 Impact upon navigation conditions of river reach between the two dams by peak shaving at Three Gorges Hydropower Station. *Procedia Engineering* **28**, 152–160.
- Zheng, S., Sun, E. & Yang, W. 2002 Study on the navigation and power station for hump modulation of Three Gorges and Gezhouba Project. *International Journal Hydroelectric Energy* **20** (2), 7–12 (in Chinese).
- Zheng, H., Zhao, Y., Tang, W., Duffield, C., Wei, Y., Huang, S. & Wu, S. 2018 A longitudinal analysis on the perspectives of major world newspapers on the Three Gorges Dam project during 1982–2015. *Water Supply* **18** (1), 94–107.
- Zhou, H.-X., Zheng, B.-Y., Meng, X.-W. & Ge, L.-Z. 2005 Influence of daily regulation of the Three Gorges Power Station on operating conditions of the approach channel. *Journal of Waterway and Harbour* **26** (1), 33–37 (in Chinese).

First received 17 August 2021; accepted in revised form 23 January 2022. Available online 4 February 2022